ACS OMEGA

Open Access

http://pubs.acs.org/journal/acsodf

Article

Near-Surfaces and Bulk Modification of Silicone Rubber under UV- and Vacuum UV-Irradiation Using Excimer and Hg Lamps

Christopher Dölle,* Christoph Schmüser, Igor Quiring, and Ralph Wilken

Cite This: *ACS Omega* 2024, 9, 45000−45010

Read Online

ACCESS | Metrics & More | Article Recommendations

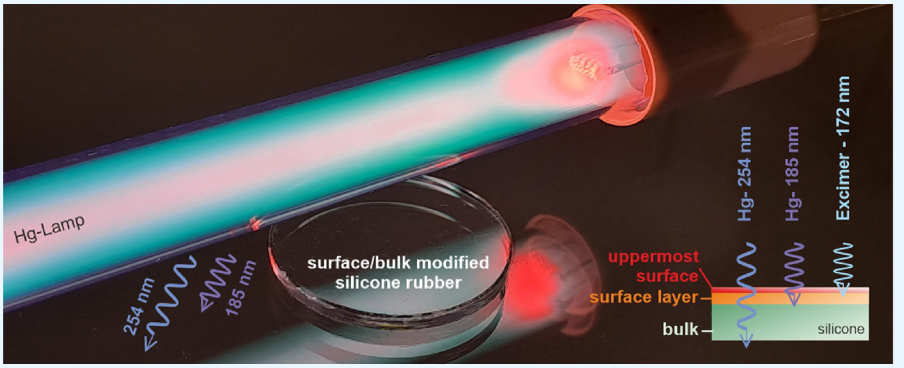

ABSTRACT: The surface properties of silicone rubber can be modified by irradiation with light from the vacuum ultraviolet (VUV) spectral range of less than 200 nm. After VUV-irradiation at 185 nm with a low-pressure mercury (Hg) lamp, a reduction in residual-dust-coverage (PA fibers) of up to 80% was found. At the same time, the long wavelength UV-radiation at 254 nm of the Hg lamp causes a reduction in the optical transmission properties of the silicone bulk. The near-surface and bulk modification of optically highly transparent silicone rubber was analyzed using XPS, ATR, transmission measurements, and investigations into the reduction of the residual-dust-coverage. A comparison was made between a Hg lamp and an excimer lamp at 172 nm. The results provide valuable information for selecting the appropriate irradiation source, depending on the desired spectral range for a given application. The results indicate that excimer lamps should be preferred for optical applications in the UV-spectral range, while Hg lamps are equally suitable for applications in the visible spectral range despite low transmission losses of less than 0.5%. The irradiation dose data were obtained using a ray tracing simulation as part of these investigations to overcome limitations of UV-sensors, such as their accelerated aging and angular dependence.

INTRODUCTION

Silicone rubber offers a versatile combination of properties that make it suitable for various industries. It exhibits biocompatibility, chemical inertness, high elasticity, and temperature stability. Some examples of its applications include medical products such as prostheses, everyday life products such as protective covers or masks, baking tins, door stoppers, and sports products. In the automotive sector, silicone is used in rain sensors and windshield wipers.

Optical silicone is a special type of silicone rubber that exhibits high transparency in the visible and UV-spectral range.[1−3] It is lighter, more flexible, and more resistant to mechanical stress compared to common glasses such as borosilicate or soda-lime, making it shatterproof. Optical silicone belongs to the liquid silicone rubber (LSR) class, known for its low viscosity in its uncured state. This enables optical silicone to be processed using injection molding, providing greater freedom in shape design.[4−6] In summary, optical silicones combine the advantages of optical glasses with those of silicone rubbers. The quality of the optical properties has reached such a high level that it can increasingly replace glass in various applications, particularly in the automotive sector for adaptive headlights.

Nevertheless, the surface properties of optical silicones are not always ideal. Its sensitivity to dust poses a challenge for optical applications as dust particles can cause scattered radiation. Aqueous cleaning is often required. Therefore, there is a significant need for a suitable surface modification process that can reduce dust attraction and facilitate easy cleaning while maintaining the optical properties of the silicone bulk.

Received: May 22, 2024
Revised: August 5, 2024
Accepted: August 16, 2024
Published: October 31, 2024

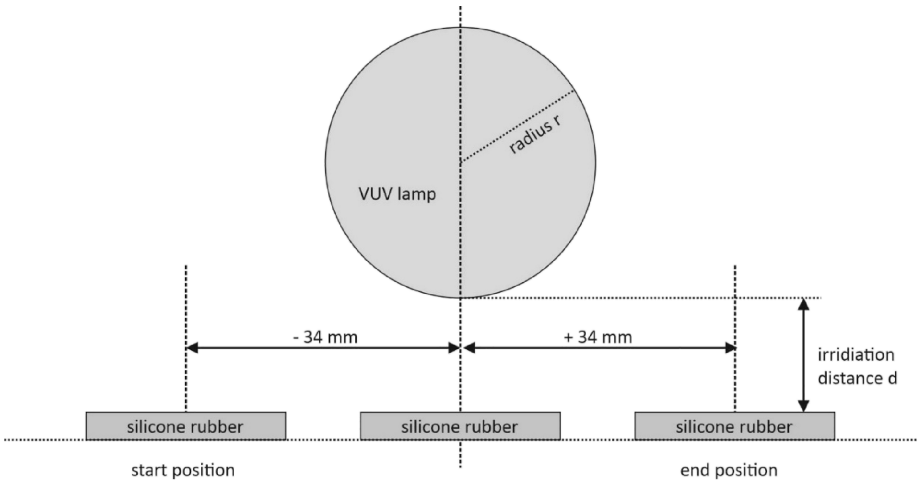

Figure 1. Silicone samples were cyclically irradiated by translating them between positions −34 and 34 mm, at a distance *d* from the lamp with radius *r*. One cycle corresponds to a travel distance of 68 mm. The ray tracing simulation also follows this model and calculates the accumulated averaged irradiation distribution for 69 evenly distributed positions for the same range.

In the state of the art, various methods for surface modification of optical silicones can be found. One common approach is gas-phase fluorination, in which hydrogen atoms are partially replaced by fluorine atoms.[7−10] However, fluorination is increasingly being viewed critically due to the use of fluorine and the formation of per- and polyfluorinated alkyl substances (PFAS) offering limited prospects for the future. Coatings such as parylene coatings have a different refractive index in comparison to the bulk material and can negatively affect the optical properties. A nonlayer-forming low-pressure plasma treatment using oxygen or ammonia as process gases can provide hydrophilic surface properties to the silicone. However, this effect is not stable over a longer period due to the migration of short-chain components.[11]

Alternatively, the surface of silicone rubber can be modified by irradiation using light of a wavelength below 200 nm (VUV, vacuum ultraviolet spectral range: 100−200 nm, VUV).[12−16] By adjusting the irradiation dose, the haptics, the surface static and dynamic friction, and dust adhesion can be specifically modified. Depending on the wavelength, the penetration depth of the radiation can reach several micrometers.[17]

There are several papers that describe the underlying effects and processes of photochemically induced conversion of poly(dimethylsiloxanes) (PDMS) for thin films by using incoherent or coherent VUV radiation. By irradiation, the methylsilane groups can be photochemically converted into silanol groups followed by degradation, resulting in the development of quartz-like properties for a thin surface layer.[12,15,18−20] The Xe*-excimer lamp[21] with emission at 172 nm and the low-pressure mercury (Hg) lamp[22] with combined VUV- and UV-radiation at wavelengths of 185 and 254 nm are the main incoherent radiation sources used for the purpose. The ratio between the radiation at 185 and 254 nm is often specified as approximately 1 to 5. Excimer lasers with emission at 193 nm (ArF) or 248 nm (KrF) are primarily used as coherent radiation sources.[23]

Optical silicones are known to exhibit high stability against UV-radiation in applications.[5,6] In completion, this work investigated the response of silicones during the modification process to the emission of commonly used VUV- and UV-light sources. A distinction was made between the changes in transmission as a silicone bulk response and ATR measurements as near-surface responses of the irradiated surfaces. XPS examinations of selected samples and microscopy were carried out to evaluate and demonstrate the effect of reduced dust adhesion, which is primarily determined by the topmost surface.

As part of these investigations, VUV- and UV- irradiation doses for 172, 185, and 254 nm were determined using ray tracing simulations to overcome the limitations of available sensors. These limitations include accelerated aging, requiring permanent calibration, and angle-dependent sensitivity, which impairs the sensor's ability to detect the total radiation energy particularly at close distances to extended light sources. Although knowing the angle-dependent sensitivity can moderate this circumstance, it still introduces some inaccuracy. Additionally, the specification of the absolute radiant power is influenced by unknown calibration conditions. Often, the absolute measurement is only reliable for a fixed position and orientation between the lamp and sensor. Finally, the ozone-generating Hg lamp's wavelengths of 185 and 254 nm complicate direct measurements, as one wavelength must be filtered out, leading to significant inaccuracies due to residual transmission and changes due to filter aging. To avoid metrological uncertainties, radiation doses given in this paper were determined by using ray tracing simulation with OpticStudio 15.5 software.

EXPERIMENTAL SECTION

Irradiation. LSR silicones (Dow Chemical Company, type Silastic TM MS-1002, thickness = 2.7 mm, diameter: 31 mm) were irradiated using a Hg lamp (uv-technik Speziallampen GmbH, Ilmenau; UVX 120 4C S 19/670 Co; radiant length 568 mm, emission at 185 and 254 nm, power at 254: 40.5 W, power at 185 nm: 8.1 W). During irradiation, the samples were moved between −34 and 34 mm relative to the lamp at a speed of 1 mm/s as shown in Figure 1. Each run is considered as one cycle. Irradiation took place in air at normal pressure and room temperature. In this series, the distance between the lamp and the silicone surface directly below the lamp at position zero was set to 5 mm. An open setup with a central exhaust was used to remove ozone. A direct ozone concentration measurement showed 15 ppm for a distance of 10 mm between the lamp and the silicone sample (ozone analyzer

https://doi.org/10.1021/acsomega.4c04823
ACS Omega 2024, 9, 45000−45010

Table 1. Compilation of the Sample Labeling and the Irradiation Parameters[a]

	sample	cycles	distance [mm]	lamp	time [s]	average185/172nm-radiation intensity [mW/cm^2]	VUV dose [J/cm^2]	average 185 nm-irradiation intensity [mW/cm2]	UV dose [J/cm2]
series 1	Si_0	0		UVX 120 S	0	0.0	0.0	0.0	0.0
	Si_4	8	5	UVX 120 S	544	6.4	3.5	35.7	19.4
	Si_6	13	5	UVX 120 S	884	6.4	5.7	35.7	31.6
	Si_8	18	5	UVX 120 S	1224	6.4	7.8	35.7	43.7
	Si_10	23	5	UVX 120 S	1564	6.4	10.0	35.7	55.8
	Si_12	28	5	UVX 120 S	1904	6.4	12.2	35.7	68.0
	Si_14	33	5	UVX 120 S	2244	6.4	14.4	35.7	80.1
series 2	Si_254 nm	22	5	UVX 40 P	1469			33.6	49.4
	Si_185_254 nm	22	5	UVX 40 S	1469	6.0	8.8	33.6	49.4
	Si_172 nm	10	5	Xeradex	680	3.5	2.4		
series 3	Si_10 mm	static	10	UVX 40 S	1000	7.8	7.8	44.5	44.5
	Si_20 mm	static	20	UVX 40 S	1592	4.9	7.8	30.6	48.7
	Si_30 mm	static	30	UVX 40 S	2364	3.3	7.8	22.4	52.9
series 4	Si_ozone	static	10	ozone at 250 ppm for 600 s					

[a]The irradiance levels were simulated using ray tracing. The value "VUV dose" refers to the radiation output at the central wavelength of 185 nm for the Hg lamp and 172 nm for the excimer lamp. "UV dose" refers to the radiation output at the central wavelength of 254 nm for the Hg lamp. The samples of series one are labeled with the corresponding 185 and 172 nm dose, the samples of series two are labeled with the applied wavelength, and series three samples are labeled with the distance between lamp and surface.

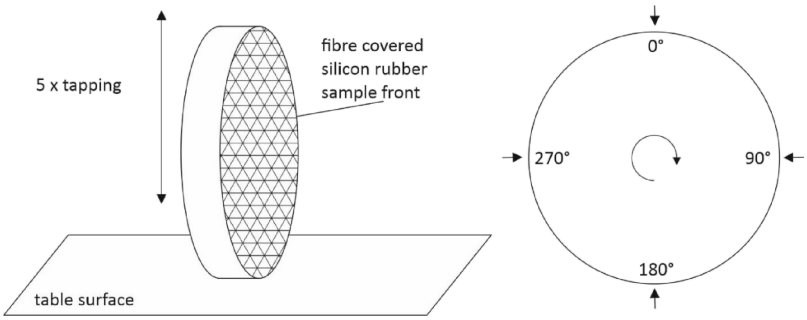

Figure 2. Procedure for removing the PA fibers from the silicone samples by tapping. Tapping the sample five times on a table surface, in vertical orientation. Rotation of the silicone by 90° each time and repetition of the tapping process.

BMT 965 ST, BMT Messtechnik GmbH, Stahnsdorf, Germany). The duration of irradiation and the number of cycles were varied. Table 1 provides an overview of the process parameters of this first test series. Sample Si_0 represents the untreated reference. The samples are labeled with the corresponding VUV-dose.

A second series of irradiation experiments were conducted using the same setup but different light sources. It involved the use of a short ozone-generating Hg lamp (uv-technik Speziallampen GmbH, Ilmenau; UVX 40 2C S 15/270 Co; radiant length 202 mm, emission at 185 and 254 nm, power at 254:13 W, power at 185 nm: 2,6 W) as well as an ozone-free Hg lamp that emits exclusively at 254 nm (uv-technik Speziallampen GmbH, Ilmenau; UVX 40 2C P 15/270 Co; power at 254 nm: 13 W). Additionally, an Xe*-excimer lamp with an emission wavelength of 172 nm was used (Radium Lampenwerk, Wipperfürth; Xeradex L40/175/SB-AZ48/93, radiant length 175 mm, power on glass surface 35 mW/cm^2).

A third series of irradiations were carried out statically at three discrete distances between the silicone surface sample and the lamp. The duration of irradiation was adjusted to ensure that the resulting irradiation dose at 185 nm was the same for all of the silicone samples. Since the sample width is smaller than the travel distance of a cycle, the average irradiance for this series is higher compared to the irradiation during translation.

Finally, a single silicone sample as series four was exposed to an oz1 atm of 250 ppm in a closed box for 10 min in order to get an impression of the surface changes of a pure ozone treatment (ozone generator: MA10K, Airthereal, Las Vegas).

Ray Tracing. The irradiance values given in Table 1 were determined using ray tracing simulations (Zemax OpticStudio 15.5). A constant air atmosphere with 21% oxygen was assumed, taking into account the oxygen absorption with σ (185 nm) = 6.17×10^{-21} cm^2, σ (254 nm) = 2.00×10^{-24} cm^2, and σ (172 nm) = 7×10^{-19} cm^2.[24−26] The simulation did not account for absorption due to ozone formation and local ozone accumulation. To simulate the irradiation distribution during the translation of the silicone samples, the simulation considered 69 positions with a constant distance of 1 mm between each position. Position zero was directly below the lamp, while the starting point was located −34 mm in front and the end point 34 mm behind the zero position; see Figure 1. The simulated total irradiation distributions for the silicone samples were accumulated for all 69 positions and finally averaged. (For additional information, see appendix A).

Residual-Dust-Coverage. To evaluate the dust adhesion, the irradiated silicone samples of the first series were completely covered with PA fibers (KSL Staubtechnik

https://doi.org/10.1021/acsomega.4c04823
ACS Omega 2024, 9, 45000−45010

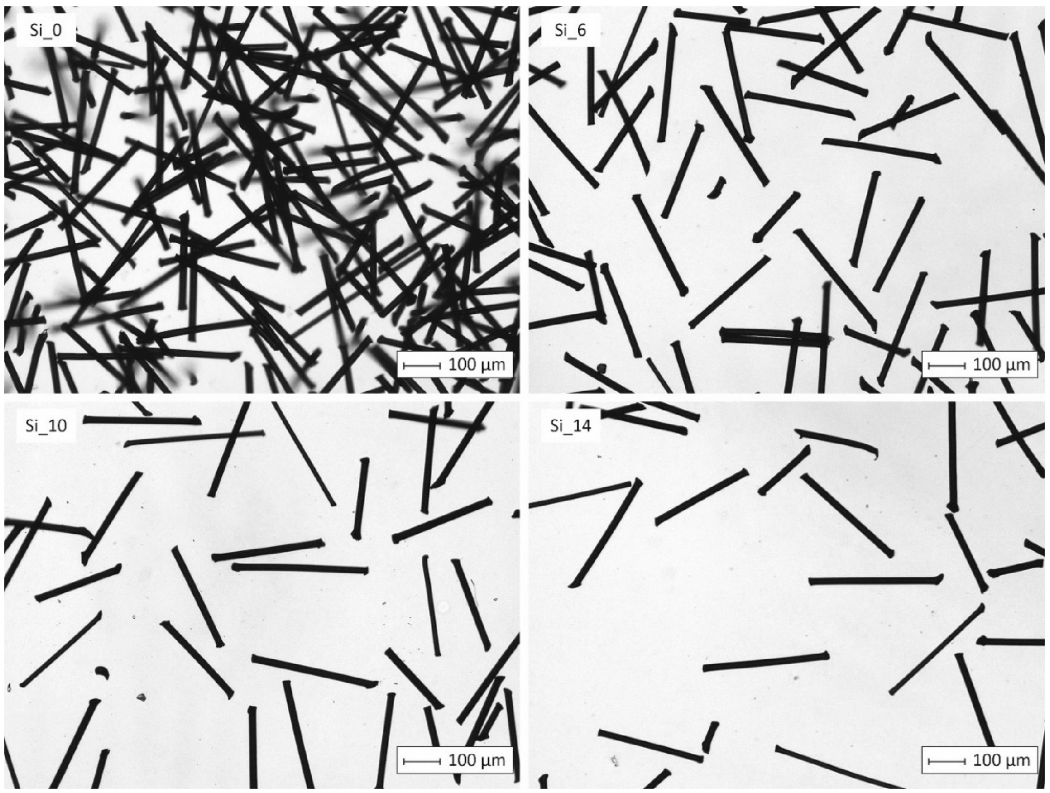

Figure 3. Microscope images for the evaluation of the residual-dust-coverage. The proportion of black fibers on the total surface area was determined. Top left: reference Si_0; top right: Si_6; bottom left: Si_10; bottom right: Si_14.

GmbH, Launingen, Germany, standard dirt polyamide fibers 3.3 dtex, 0.3 mm average length, black). Subsequently, the fibers were removed by manual tapping of the silicone on a table in such a way that the dirt-covered sample was aligned vertical to the table surface, see Figure 2. The tapping itself was repeated five times. This entire procedure is repeated four times, rotating the silicone sample by 90° each time. Finally, the percentage of the surface area still covered with residual fibers is determined. Images were captured and analyzed using a microscope (KEYENCE DEUTSCHLAND GmbH, Neu-Isenburg, VHX600). The observed area measured at least 1 mm × 1 mm. The evaluation was performed at five different, nonoverlapping positions on the irradiated silicone surface.

UV−vis-Transmission Measurements. A UV−vis measuring device (SPECORD 210 PLUS, Analytic Jena GmbH, Jena) was used to measure the transmission in the wavelength range from 320 to 800 nm. This device is a dual-beam photometer, where air was measured as a reference in the first channel, while the transmission of the silicone sample was measured in the second channel. The reference arm was calibrated to air with a constant transmission value of 100%. The measuring spot had a diameter of approximately 10 mm. The measuring speed was set to 5 nm/s, and both the slit width and step width were set to 1 nm.

ATR Surface Analysis. One method of characterizing surface chemistry is given by the ATR (attenuated total reflection) measurement. ATR utilizes total internal reflection and provides a chemical fingerprint of the investigated surface layer. The information depth is given by the penetration depth and is approximately 0.5 to 2 μm. In this study, an ATR instrument from Bruker (Bruker Corporation, Bremen, Bruker Alpha II, Platinum ATR, and Diamond Crystal) was used. A total of 32 spectra were recorded in the range of 4000−600 cm^{-1} with a spectral resolution of 1 cm^{-1}. Air was used as the background.

XPS Analysis. The photochemical-induced conversion of PDMS to a SiO_x-like layer is subjected to a modification of the chemical composition of the irradiated layer.[14] X-ray photoelectron spectroscopy (XPS) is a widely used technique for surface-sensitive quantitative analysis of surface chemistry, excluding hydrogen and helium. In this study, XPS was performed using a Kratos Axis Ultra spectrometer (Kratos Analytical Corp.). The method has high detection sensitivity with an element-specific sensitivity of about 1,000 ppm. The typical depth of information obtained is approximately 10 nm. The peaks of O 1s, Si 2p, and C 1s were used to determine the atomic amounts of oxygen, silicon, and carbon, respectively. The results presented are the averages of two individual measurements taken at different positions on the same sample.

RESULTS

Reduction in Residual-Dust-Coverage. Figure 3 shows representative microscope images of the silicone rubber surface from the first irradiation series after tapping. The effect of a reduced residual-dust-coverage for irradiated silicone surfaces (185 and 254 nm) is evident. The reference sample exhibits a residual-dust-coverage of approximately 40%, whereas it decreases to 15.5% for a 185 nm irradiation dose of 5.7 J/cm^2 (sample Si_6). At a 185 nm dose of 10 J/cm^2, the average residual-dust-coverage is approximately 9.8%, and at 14.4 J/cm^2, it is 7.2%. The overall evaluation, illustrated in Figure 4, demonstrates a consistent residual-dust-coverage reduction of at least 60% for all irradiated samples compared to the reference. The coverage decreases continuously with higher

https://doi.org/10.1021/acsomega.4c04823
ACS Omega 2024, 9, 45000−45010

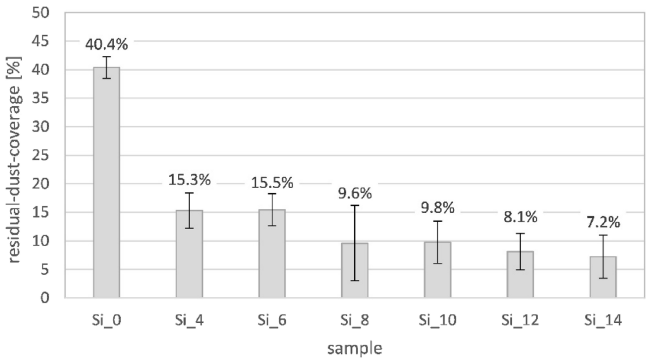

Figure 4. Residual-dust-coverage after tapping the PA fibers, expressed as a percentage of the total surface area for the first irradiation series. Each measuring point comprises five measurements at different positions on the silicone rubber sample. The sample label on the *x*-axis corresponds to the simulated 185 nm irradiation dose.

185 nm irradiation doses. For doses above 10 J/cm^2, the reduction is 75% or higher. Figure 5 presents the results of the

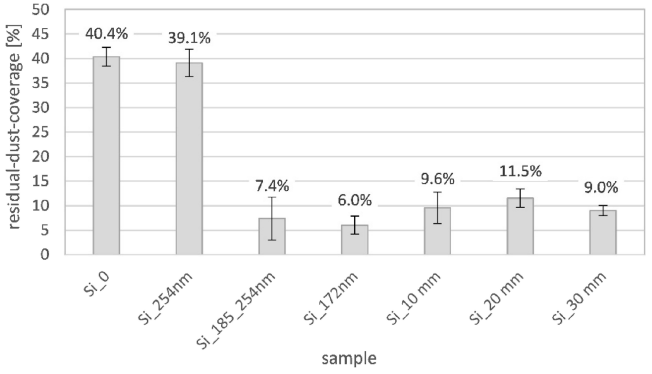

Figure 5. Residual-dust-coverage after tapping the PA fibers, expressed as a percentage of the total surface area for the second and third irradiation series. The sample labels on the *x*-axis indicate the applied wavelengths (series two) and the distance between lamp and surface (series three). Si_0 is the untreated reference.

residual-dust-coverage for the second and third irradiation series. The residual-dust-coverage after pure 254 nm irradiation with a UV-dose of 49.4 J/cm^2 remains unchanged and almost identical to the reference. In contrast, when exposed at the identical 254 nm dose of 49.4 J/cm^2 but combined with 185 nm/254 nm irradiation (185 nm dose: 8.8 J/cm^2), the residual-dust-coverage is significantly reduced by 92.6%. When irradiated with the excimer lamp at a wavelength of 172 nm, the residual-coverage is even reduced by 94.0%. In addition, the samples Si_10 mm, Si_20 mm, and Si_30 mm, which were irradiated at the same VUV- but different UV-dose, are at a comparable level within the measurement deviation showing a residual-dust-coverage of 10%.

Transmission. In Figures 6 to 9, the transmission measurements for the first three irradiation series are shown. To ensure clarity, only the values of the samples Si_4, Si_8, and Si_14 and the reference are shown representing the first irradiation series in Figure 6. In the long-wavelength spectral range, the transmission of the untreated reference compared to air is approximately 93−94%. In the short-wavelength spectral range, the transmission drops to approximately 87%. The transmission decreases continuously with shorter wavelengths

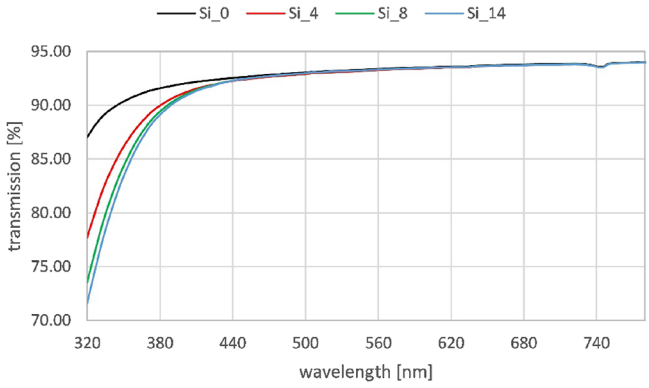

Figure 6. Absolute transmission for a selection of silicone samples from the first irradiation series with variation of the 185 and 254 nm irradiation dose. Air, with a constant transmission of 100%, serves as the reference. The sample label corresponds to the simulated VUV-irradiation dose.

and higher irradiation doses, as shown in Figure 6 and the transmission data for 320 nm in Figure 7 for the complete first

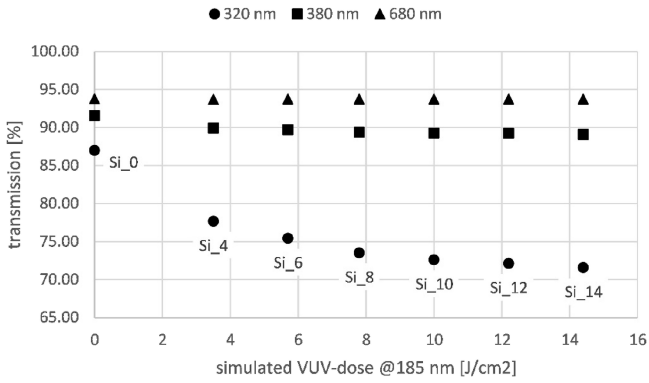

Figure 7. Absolute transmission for the first irradiation series varying the 185 nm and 254 nm irradiation dose at discrete wavelengths of 320, 380, and 680 nm.

series. At 745 nm, material-specific absorption is observable but not relevant in this context. As shown in Figure 7 and in Table 2 explicitly for the wavelengths 320, 380, and 680 nm, the transmission decreases with higher 185 nm or 254 nm irradiation doses. The lowest value recorded for a 185 nm irradiation dose of 14.4 mJ/cm^2 (254 nm: 80.1 mJ/cm^2) for the wavelength 320 nm is 71.59%, representing a 15% decrease compared to the reference. Table 2 also shows the average absolute transmission in the visible spectral range from 380 to 780 nm and the relative transmission compared with the reference in the same spectral range. The reduction in transmission in the visible spectral range, compared to the untreated silicone, is therefore less than half a percent.

Figure 8 displays the absolute transmission in the spectral wavelength range from 320 to 350 nm of the silicone samples for the second irradiation series, where the light source was varied, and for the pure ozone treatment. It can be observed that the transmission remains almost identical to that of the reference after irradiation at 172 nm. The transmission under combined irradiation with 185 and 254 nm closely matches the transmission for pure UV-irradiation at 254 nm using the same UV-dose of 49.4 mJ/cm^2. In contrast, in the third irradiation series, applying the same 185 nm dose (7.8 J/cm^2), the

https://doi.org/10.1021/acsomega.4c04823
ACS Omega 2024, 9, 45000−45010

Table 2. Absolute and Relative Transmission Values for the First Irradiation Series Varying the 185 and 254 nm Irradiation Dose[a]

sample	Si_0	Si_4	Si_6	Si_8	Si_10	Si_12	Si_14
transmission at 320 nm	87.01	77.70	75.46	73.54	72.62	72.15	71.59
transmission at 380 nm	91.59	89.96	89.71	89.41	89.28	89.25	89.11
transmission at 680 nm	93.78	93.72	93.74	93.72	93.72	93.72	93.72
average transmission380−780 nm	93.26	93.07	93.10	93.07	93.06	93.06	93.05
relative transmission 380−780 nm	100.00	99.79	99.82	99.79	99.78	99.79	99.77

[a]Lines 1 to 3 show the transmission for single wavelengths. Line 4 shows the average values of all single measurements in the specified spectral range, recorded with a 1 nm step size and using air as the reference. Line 5 presents these values relative to the unirradiated silicone reference, Si_0.

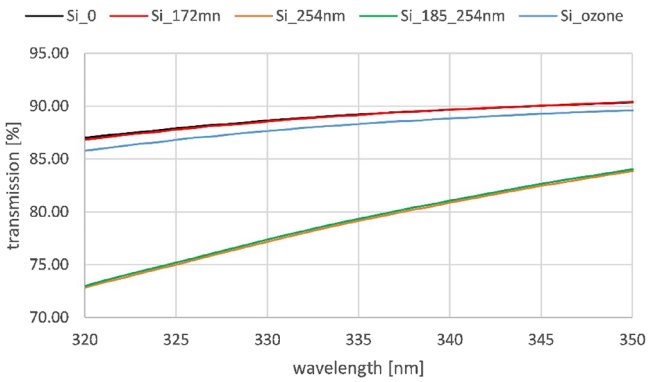

Figure 8. Absolute transmission in the spectral range from 320 to 350 nm for the second irradiation series varying the light source and the irradiation wavelength for the pure ozone treatment. The transmission curve for the samples Si_0 and Si_172 nm are almost congruent, and the same applies to the transmission curve for the samples Si_254 nm and Si_185_254 nm.

transmission data reveal a reduced transmission with increasing 254 nm dose, see Figure 9. A pure ozone treatment introduces a small reduction in the transmission of 1%, see Figure 8.

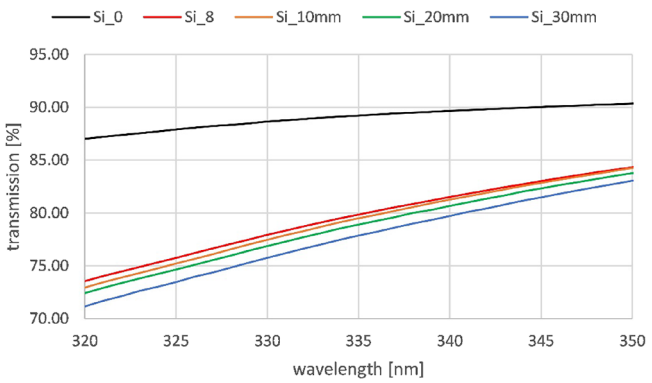

Figure 9. Absolute transmission in the spectral range from 320 to 350 nm for the reference Si_0 and sample Si_8 (first irradiation series) compared to the samples of the third irradiation series, varying the distance at a constant 254 nm irradiation dose.

ATR Surface Analysis. The ATR spectra are categorized into different wavenumber ranges; see Figures 10 to 14. Figure 10 shows representative spectra for the first irradiation series. The nonirradiated silicone rubber reference exhibits typical symmetric and asymmetric stretching vibrations of the methyl groups at wavenumbers 2906 cm^{-1} ($\nu_s(CH_3)$) and 2963 cm^{-1} ($\nu_{as}(CH_3)$).[15] As the methyl groups are replaced by oxygen during irradiation, the intensities of these bands decrease with increasing 185 nm irradiation dose. Concurrently, a broad

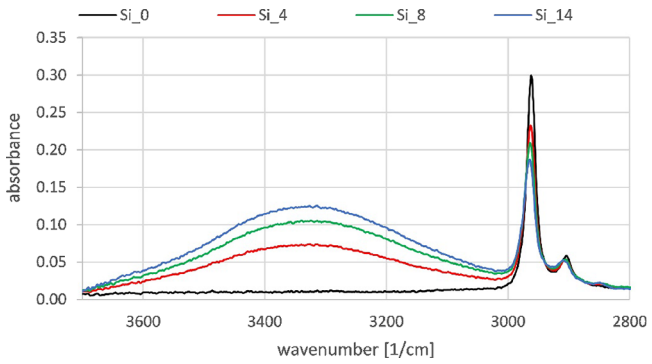

Figure 10. Exemplary ATR spectra for the first irradiation series varying the 185 and 254 nm irradiation dose in the wavenumber range from 2800 to 3700 cm^{-1}.

band emerges at 3300 cm^{-1}, which intensifies with the 185 nm irradiation dose. This band can be assigned to the symmetrical stretching vibration ν_s(OH), indicating the formation of hydroxyl groups.[15,27] Additionally, absorption bands in the range of 2800−3500 cm^{-1} are expected due to water trapped in the layer.[28,29]

Figure 11 illustrates the wavenumber range from 950−1150 cm^{-1}. Various asymmetric stretching vibrations of the Si−O−

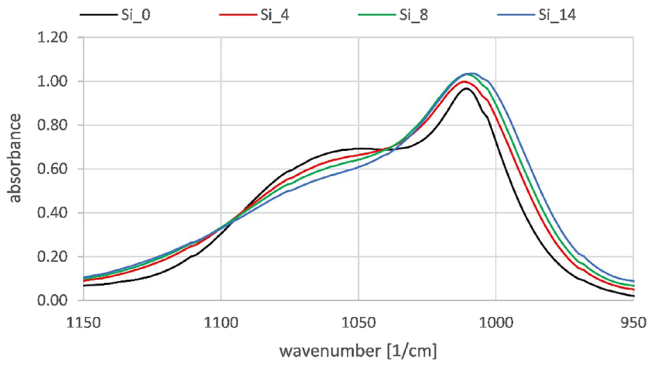

Figure 11. Exemplary ATR spectra for the first irradiation series varying the 185 and 254 nm irradiation dose in the wavenumber range 950 to 1150 cm^{-1}. The sample label corresponds to the simulated 185 nm irradiation dose.

Si unit (ν_{as} (Si−O−Si)) are localized in this range.[15,16,30,31] 185 nm irradiation affects the intensity ratio between these bands. As the irradiation dose increases, the absorbance of the band around 1010 cm^{-1} increases while the intensity of the shoulder around 1060 cm^{-1} decreases slightly. In a study involving 200 nm thin PDMS films, the authors even observed a shift from 1111 to 1231 cm^{-1} through IRRAS measurements, along with an increase in the intensity of the band with the

https://doi.org/10.1021/acsomega.4c04823
ACS Omega 2024, 9, 45000−45010

highest absorbance, while the intensity of the shoulder decreased significantly, consistent with the available data of Dölle et al.[14]

Finally, Figure 12 presents the absorption band for the symmetric deformation vibration $\delta_s(CH_3)$, which is localized

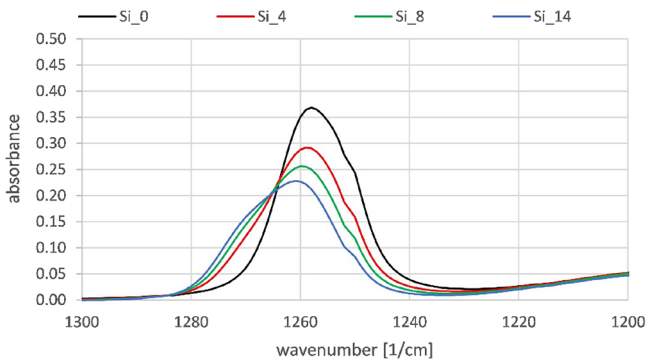

Figure 12. Exemplary ATR spectra for the first irradiation series varying the 185 and 254 nm irradiation dose in the wavenumber range 1200 to 1300 cm^{-1}.

around 1258 cm^{-1} for the reference.[15,32,33] As the 185 nm irradiation dose increases, the intensity of the band decreases, and it shifts toward 1261 cm^{-1}. It is known that this band can shift to 1280 cm^{-1} for thin film irradiation.[14,15] The shift of the $\delta_s(CH_3)$ vibration indicates a change of the structural unit from $-O-Si(CH_3)_2-O-$ to $-O-Si(CH_3)(O^-)_2$ caused by cross-linkage of chains and by the replacement of methyl by hydroxyl-groups, as reported in the literature.[15] In thin silicone films, a high irradiation dose can cause this band to disappear completely once all CH_3 side chains have been removed by fragmentation.

Figure 13 shows the ATR spectra for the second series of measurements in the range 2800−3700 cm^{-1}. The spectra for

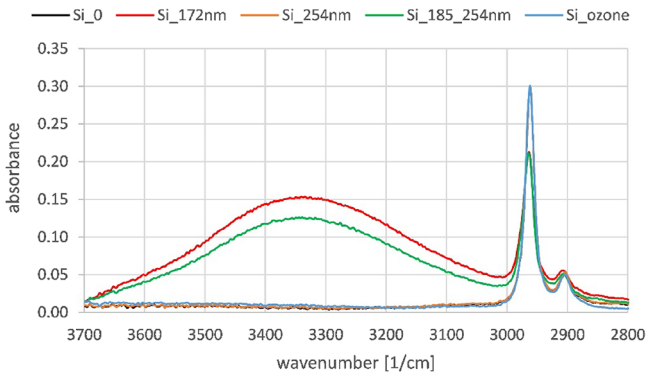

Figure 13. ATR spectra for the second irradiation series and for pure ozone-treated sample for different light sources in the wavenumber range 950 to 1150 cm^{-1}. The spectra for the samples Si_0, Si_254, and Si_ozone are almost congruent.

the reference and the Si_254 nm sample are almost identical, even in the wavenumber range not explicitly shown. In contrast, the spectra for excimer irradiation show more pronounced typical changes of the first series of irradiation. The third irradiation series shows three identical spectra within the measurement accuracy, see Figure 14. All three spectra show the same qualitative changes in the spectrum that were observed for irradiation series one.

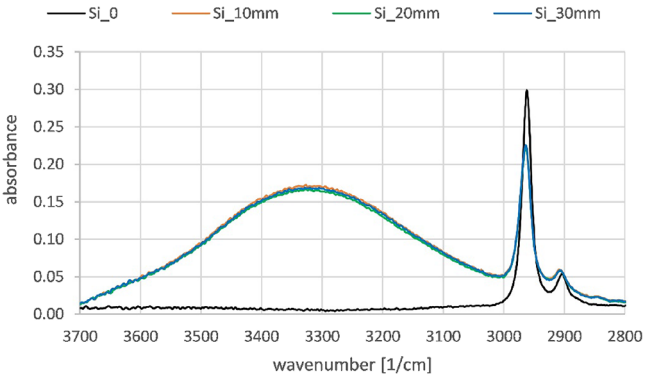

Figure 14. ATR spectra for the third irradiation series for constant 185 nm irradiation dose in the wavenumber range 2800 to 3700 cm^{-1}. The spectra for the samples Si_10 mm, Si_20 mm, and Si_30 mm are almost congruent.

XPS Analysis. In Table 3, the XPS elemental analysis of the third irradiation series compared with the reference for the

Table 3. XPS Elemental Analysis of the Chemical Composition of the Silicone Surfaces before and after Irradiation with a Constant 185 nm Dose of 7.8 J/cm^2 but Different 254 nm Dose (see Table 1)

	C 1s	O 1s	Si 2p
sample	[at. %]	[at. %]	[at. %]
Si_0	43.4 ± 0.14	29.6 ± 0.28	27.0 ± 0.00
Si_10 mm	22.1 ± 0.28	49.6 ± 0.42	28.4 ± 0.07
Si_20 mm	21.7 ± 0.14	50.0 ± 0.00	28.3 ± 0.14
Si_30 mm	21.4 ± 0.28	50.3 ± 0.42	28.4 ± 0.07

elements oxygen, silicon, and carbon can be seen. The analysis reveals a significant increase in oxygen by 20 at. %, while the carbon content decreases from 43 at. % to approximately 22 at. %. The silicon proportion remains nearly unchanged at around 28 at. %. All three irradiated silicone rubber samples exhibit an element distribution that is identical within the measurement accuracy.

DISCUSSION

The UV- and VUV-irradiation doses at 172, 185, and 254 nm were simulated using ray tracing due to the limitations of available power meters for direct measurement as mentioned before. It is important to acknowledge that simulation also has specific limitations. Primarily, the used software does not account for time dependencies, such as local or temporal inhomogeneities within the gas discharge, nor does it capture temperature fluctuations in the atmosphere, which can significantly affect the output of the Hg lamp. Direct measurement, in contrast, would always show real-time data.

On the one hand, for the simulation, it was necessary to assume that the gas atmosphere composition stays constant, specifically an air atmosphere with 21% oxygen content. Direct measurement of the ozone concentration using the ozone analyzer showed a time constant ozone level of 15 ppm at a 10 mm distance from the Hg lamp, which is much lower compared to the oxygen concentration. The ozone concentration theoretically reduces the irradiation power by approximately 0.03% at 185 nm ($\sigma = 6.7 \times 10^{-19}$ cm^2) and 0.4% at 254 nm ($\sigma = 1.18 \times 10^{-17}$ cm^2[24−26]), which is classified as a minor inaccuracy. For irradiation series one and

https://doi.org/10.1021/acsomega.4c04823
ACS Omega 2024, 9, 45000−45010

two, the absolute radiant intensity is of minor importance compared to the relative change. For the third irradiation series, it is crucial to match the absolute values as accurately as possible. To improve the simulation's accuracy, further studies should consider optimizing the gas composition. To enhance the simulation accuracy, future studies should focus on optimizing the gas composition. However, ozone formation and depletion are considered strong dynamic processes, with dependencies currently unknown to the authors.

On the other hand, to enhance accuracy, the simulation software accounts for changes in spectrum distribution with distance due to the spectral-depending absorption coefficient of oxygen. Therefore, the emission spectrum is always simulated by using three wavelengths: the central emission wavelength and the wavelengths at which the intensity has dropped to 1/e. For the excimer lamp, the wavelengths are 158, 172, and 186 nm with the weighting 1/e:1:1/e. For the Hg lamp, these wavelengths are 184, 185, and 186 nm. Especially in the spectral range around 185 nm, this averaging strategy will help to reduce the uncertainty in reading the absorption values due to the strong changes in coefficient in the Schumann−Runge bands.

The XPS results in Table 3 confirm the light induced transformation, which fits perfectly with the changes in elemental composition and absorbance changes described in the literature. The limited information depth of the XPS analysis (10 nm) allows for a comparison between the data presented here for thick silicone samples (2.7 mm) and the data from the authors' previous measurements on 200 nm thin PDMS layers.[14] The silicone samples modified here with a residual surface carbon content of 20 at. % can be classified as moderately cross-linked. Intense modified PDMS layers can have a residual carbon content below 5 at. %.[15]

The relative measurement deviation of up to 50% for residual-dust-coverage is primarily attributed to manual tapping. This method was chosen for reasons of simplicity and is certainly not the most quantitative technique. Nevertheless, a significant reduction in residual-dust-coverage is clearly detectable. Additionally, the results in Figure 4 show a significant tendency for residual-dust-coverage to decrease with higher 185 nm irradiation doses. Due to the higher silicone absorption coefficient at shorter wavelengths, it can be assumed that a lower irradiation dose is needed when using the excimer lamp at 172 nm compared to the Hg lamp to achieve a comparable grade of surface cross-linking. Comparing the Si_185_254 nm and Si_254 nm samples reveals that an ozone-free Hg lamp with pure emission at 254 nm is ineffective in reducing dust-coverage, even when applying the same 254 nm irradiation dose. Therefore, the hypothesis can be derived that solely the 185 nm wavelength dominates the near-surface modification of the silicone, which is crucial for its topmost surface properties. This assumption is confirmed using an excimer lamp, which does not emit UV-radiation but still creates similar surface properties. The hypothesis is further supported by the ATR analysis: Figure 13 shows the typical changes in absorption bands toward a SiO_x-like layer after irradiation with 172 nm or the combined irradiation with 185 and 254 nm from the Hg lamp. In contrast, Hg lamp irradiation exclusively at 254 nm shows no detectable changes in band positions and intensities compared to the reference, despite applying the same 254 nm dose. Further proof is given by the highly surface-sensitive XPS analysis in Table 3: Despite varying the working distance and the 254 nm dose, the results consistently yield nearly identical results in accordance with the constant 185 nm irradiation dose. Therefore, the changes in ATR spectra, elemental composition detected by XPS, and the decrease in residual-dust-coverage are directly correlated with the 185 nm dose, not with the 254 nm dose. As an example, Figure 12 depicts the correlation between the 185 nm irradiation dose and changes in the absorbance for a representative wavenumber region, indicating the formation of a SiO_x-like layer in accordance with the literature. The same simultaneous decrease in residual-dust-coverage can be seen in Figure 5.

The difference in response of the silicone rubber to the 172, 185, and 254 nm light is reflected in the penetration depths into silicone. The penetration depth for 172 nm is approximately 0.1 μm ($\alpha \sim 7.7$ to 10.4 μm^{-1}). It is 1 order of magnitude higher for 185 nm at approximately 0.7−1.0 μm ($\alpha \sim 0.9$ to 1.4 μm^{-1}).[17,34,35] Around 254 nm, the penetration depth increases significantly to approximately 11 mm ($\alpha \sim 0.2$ to 2 cm^{-1}), several orders of magnitude higher.[2,36,37]

The analysis of the transmission provides further insight: Looking at Figure 8, it is suggested that the reduction in transmission is essentially determined by the 254 nm irradiation dose. The transmission after irradiation with only 254 nm is almost identical to the transmission after irradiation with combined irradiation of 185 and 254 nm. Irradiation with 172 nm shows no significant change compared with the reference. Therefore, the second hypothesis is that reduction in transmission of the silicone bulk is caused by the UV light. This assumption is confirmed by Figure 9, where samples with the same 185 nm dose exhibit different transmissions that decrease with the 254 nm dose. The modification of the silicone to an inorganic SiO_x by 185 nm irradiation is limited to a thin surface layer due to the low penetration depth. This thin layer, several micrometers thick, makes only a small contribution to the transmission measurement compared to the bulk, which had a thickness of 2.7 mm. In contrast, the 254 nm irradiation penetrates deeper into the silicone and interacts with it, creating color centers that reduce transmission in correlation with the applied 254 nm dose. The correlation is clearly visible in Figures 6 and 7, and particularly in Figure 9, where the 185 nm irradiation dose was held constant. The reduction in transmission depends on the wavelength and increases significantly with shorter wavelengths. According to Table 2, in the visible spectral range from 380 to 780 nm, the difference in the average transmission compared to non-irradiated silicone is less than 0.5%, even at the highest 254 nm dose. However, at 320 nm, the reduction in transmission can be as high as 15%.

All observed changes in silicone properties result from either direct light−silicone interaction or indirect interaction between reactive oxygen species, such as ozone or atomic oxygen, and the silicone surface. The dominant interaction cannot be conclusively determined in these investigations. The reduction in transmission by over 10% around 320 nm is already observed for the ozone-free Hg lamp (see Figure 8), indicating that irradiation at 254 nm is primarily responsible. No additional effect is recognizable for the combined 185 and 254 nm irradiation, even though the identical 254 nm dose with the ozone-generating Hg lamp within the measurement accuracy was used and ozone was present. Both the generated ozone and the 185 nm radiation do not appear to cause any further reduction in transmission. However, an ozone-related effect cannot be entirely excluded, as the pure ozone treatment

https://doi.org/10.1021/acsomega.4c04823
ACS Omega 2024, 9, 45000−45010

results show a significant 1% reduction. The ozone concentration at 250 ppm in this measurement is an order of magnitude higher compared to the irradiation, potentially amplifying the ozone effect, which cannot be clearly observed at 15 ppm. No effect of pure ozone treatment was observed in the surface-sensitive ATR measurement (see Figure 13).

Additionally, silicone may be modified by atomic oxygen. The radiation at 185 nm of the ozone-generating Hg lamp effectively generates ozone, which, following the Chapman cycle describing the ozone generating and depletion, ensures an increased ratio of atomic oxygen in interaction with 254 nm radiation. This suggests that changes in surface-sensitive ATR and XPS measurements may result from both direct light−silicone interactions and indirect interactions with atomic oxygen, or even a mixture of both reactions. Since XPS analysis primarily indicates significant carbon reduction due to fragmentation and an oxygen increase, it cannot be excluded that both interactions might be responsible for the observed silicone modifications. However, the results for 172 nm radiation, which show very similar modifications but lack the 254 nm component accelerating ozone depletion and atomic oxygen formation, indicate a dominant influence of the radiation. Further analysis requires increased measurement efforts due to the extremely short lifetime of atomic oxygen, which, unfortunately, was not available.

SUMMARY AND OUTLOOK

Optical silicones, known for their high transparency in the visible spectral range, serve as an excellent alternative to glass in various applications.[36,38−40] The investigations conducted confirm that the surface properties of silicones can be modified by light in the VUV-spectral range below 200 nm, resulting in a significant reduction in residual-dust-coverage. It has been demonstrated that there are distinct differences between 254, 185, and 172 nm irradiation when it comes to modifying silicone rubber with light. These differences can be attributed to the penetration depth of the light. VUV-light at 185 or 172 nm penetrates only a few micrometers into the silicone, imparting glass-like properties to the topmost surface, which is mainly responsible for the dust adhesion and residual-dust-coverage. This modification can be quantitatively confirmed and analyzed using surface-sensitive measurement techniques such as XPS or ATR. On the other hand, 254 nm light penetrates several millimeters into the silicone and does not induce modification of the uppermost surface. Instead, a bulk reaction can be observed, resulting in reduced transmission, which is not observed with 172 or 185 nm light. For a precise understanding, it will be necessary to analyze the color centers and their formation in more detail.

The findings are highly valuable for users who need to choose an appropriate irradiation source. Surface modification cannot be achieved with pure UV-irradiation (254 nm). The observed trends can guide a targeted selection between the commonly used sources of a Hg lamp (185 and 254 nm) and an excimer lamp (172 nm). The user must identify the best compromise between surface effect, modification depth, and transmission loss for their specific application. It should be noted that a moderate 172 or 185 nm irradiation dose is often sufficient to achieve desired surface effects. However, it is important to consider that the modified surfaces may develop crack structures under mechanical stress.[41] In order to evaluate the correlation among wavelength, irradiation dose, and the development of cracks in optical silicone, further detailed research is needed. However, there are existing papers that provide initial insights.[41,42]

In the case of optical applications, it is important to consider that 254 nm irradiation can result in a loss of transmission. In the visible spectral range, the reduction caused by 254 nm light is less than 0.5% compared to untreated silicone. In the UV-spectral range, the reduction can be significantly higher, up to 15%. Therefore, the choice of the appropriate light source for surface modification depends on the specific spectral requirements of the application. For optical applications located in the visible spectral range, both light sources, Hg lamps and excimer lamps, can be used. For applications in the UV-spectral range, the excimer lamp is more suitable as it does not emit UV radiation that causes transmission losses of the optical silicones in the UV-spectral range. Unfortunately, conventional Hg lamps have an unfavorable 254 nm emission that is almost five times more intense than the 185 nm emission. It would be desirable to control the 254 nm-to-185 nm ratio of a Hg lamp, for example, by using filters or special process gases, or to develop new pure VUV-light sources for future advancements.

APPENDIX A

Some additional information for the ray tracing simulation.

The simulation software used was OpticStudio, version 15.5 (Zemax LLC, Ansys Inc.) running in nonsequential mode. Lamps were modeled based on manufacturers' specifications, using Suprasil 110 as quartz glass with a thickness of 0.5 mm. No radiation reabsorption occurred within the quartz cylinder during simulation. To optimize calculation time, the simulated lamp length was limited to 150 mm, adequate compared to the 31 mm silicone samples, allowing edge effects at the lamp socket to be neglected. The radiant power per cm was adjusted in the simulations for each specific lamp and wavelength:

UVX 120 (Ø = 19 mm): 0.71 W/cm (254 nm) 0.14 W/cm (185 nm)

UVX 40 (Ø = 15 mm): 0.64 W/cm (254 nm) 0.13 W/cm (185 nm)

Xeradex L40/175 (Ø = 40 mm): 0.44 W/cm (172 nm)

Each lamp was classified as a volume radiator (object type: Source Volume Cylinder) in the simulation, which assumed at least 1,000,000 point light sources (Analysis Rays) within the cylinder, emitting in random directions.

To simulate irradiance on the silicone sample, the sample surface was modeled as a rectangular detector (object type: Detector Rectangle) with a side length of 31 mm and a pixel resolution of 1 mm, recording the incoherent irradiance using a 180° sensitivity angle. Finally, a rectangular volume of 240 mm × 160 mm × 1500 mm in size was placed surrounding the arrangement consisting of lamp and silicone to define the gas atmosphere (object type: rectangular volume). The translation path of the silicone sample between −34 and +34 mm was divided into 69 single simulation steps, shifting the detector by 1 mm per step (see Figure 1). The simulation accumulated the data from all steps, averaging the irradiation dose values by dividing by 69.

Simulation (Ray trace) parameters included "Use Polarization", "Ignore Errors", "Split NCS Rays", and "Scatter NSC Rays" to address beam refraction and scattering effects.

AUTHOR INFORMATION

Corresponding Author

Christopher Dölle − *Fraunhofer Institute for Manufacturing Technology and Advanced Materials IFAM, Bremen 28359,*

https://doi.org/10.1021/acsomega.4c04823
ACS Omega 2024, 9, 45000−45010

Germany; orcid.org/0009-0000-5784-2952;
Email: Christopher.doelle@ifam.fraunhofer.de

Authors

Christoph Schmüser − *Fraunhofer Institute for Manufacturing Technology and Advanced Materials IFAM, Bremen 28359, Germany*

Igor Quiring − *Fraunhofer Institute for Manufacturing Technology and Advanced Materials IFAM, Bremen 28359, Germany*

Ralph Wilken − *Fraunhofer Institute for Manufacturing Technology and Advanced Materials IFAM, Bremen 28359, Germany*

Complete contact information is available at:
https://pubs.acs.org/10.1021/acsomega.4c04823

Author Contributions

Conceptualization: C.D., C.S., R.W. Methodology: C.D., C.S., I.Q., R.W. Validation: C.D., C.S., I.Q., R.W. Formal analysis: C.D., R.W. Investigation: C.D., C.S., R.W. Resources; C.D., C.S., I.Q., R.W. Data curation: C.D., C.S., I.Q., R.W. Writing—original draft preparation: C.D. Writing—review and editing: C.D., C.S., I.Q., R.W. Visualization: C.D. Supervision: C.D., R.W. Project administration: C.D., C.S. All authors have read and agreed to the published version of the manuscript.

Notes

The authors declare no competing financial interest.

■ ACKNOWLEDGMENTS

Thanks are given to our Fraunhofer Institute for Manufacturing Technology and Applied Materials Research, IFAM, for making this research possible.

■ REFERENCES

(1) Gu, Q. G.; Zhou, Q. L. Preparation of high strength and optically transparent silicone rubber Eur. *Polym. J.* **1998**, *34* (11), 1727−1733.
(2) Li, W.; Huber, G. M. Optical characterization of RTV615 silicone rubber compound. *J. Instrum.* **2014**, *9*, P07012.
(3) Zhao, C. H. An all-silicone zoom lens in an optical imaging system. *Chin. Phys. B* **2013**, *22* (9), No. 094214.
(4) Kuo, C. C.; Lin, J. X. Fabrication of the Fresnel lens with liquid silicone rubber using rapid injection mold. *J. Adv. Manuf. Technol.* **2019**, *101*, 615−625.
(5) Hopmann, C.; Röbig, M. Injection moulding of high precision optics for light-emitting diodes made of liquid silicone rubber. *J. Elastomers Plast.* **2017**, *49* (1), 62−76.
(6) Bont, M.; Barry, C.; Johnston, S. A review of liquid silicone rubber injection molding: Process variables and process modeling Polym. *Eng. Sci.* **2021**, *61* (2), 331−347.
(7) An, Z.; Shan, F.; Yang, L.; Shen, R.; Gu, X.; Zheng, F.; Zhang, Y. Unusual effect of temperature on direct fluorination of high temperature vulcanized silicone rubber and properties of the fluorinated surface layers. *Dielectr. Electr. Insul.* **2018**, *25* (1), 190−198.
(8) Du, B. X.; Li, Z. L.; Li, J. Surface charge accumulation and decay of direct-fluorinated RTV silicone rubber. *IEEE Trans. Dielectr. Electr. Insul.* **2014**, *21* (5), 2338−2342.
(9) Chen, T.; Shen, Z.; An, Z.; Zheng, F.; Zhang, Y. Effect of Direct Fluorination on Tracking and Erosion Resistance of Liquid Silicone Rubber. *IEEE Int. Conf. High Voltage Eng. Appl.* **2020**, 1−4.
(10) Shen, Z.; An, Z.; Chen, T.; Wang, X.; Zheng, F.; Zhang, Y. Simultaneous Improvement of Surface Properties of the Liquid Silicone Rubber by Direct Fluorination. *IEEE 3rd Int. Conf. Dielectr.* **2020**, 150−153.
(11) Fritz, J. L.; Owen, M. J. Hydrophobic recovery of plasma-treated polydimethylsiloxane. *J. Adhes.* **1995**, *54* (1−4), 33−45.
(12) Schnyder, B.; Lippert, T.; Kötz, R.; Wokaun, A.; Graubner, V.-M.; Nuyken, O. UV-irradiation induced modification of PDMS films investigated by XPS and spectroscopic ellipsometry. *Surf. Sci.* **2003**, *532*, 1067−1071.
(13) Mirley, C. L.; Koberstein, J. T. A Room Temperature Method for the Preparation of Ultrathin SiOx Films from Langmuir-Blodgett Layers. *Langmuir* **1995**, *11* (4), 1049−1052.
(14) Dölle, C.; Papmeyer, M.; Ott, M.; Vissing, K. Gradual photochemical-induced conversion of liquid polydimethylsiloxane layers to carbon containing silica coatings by VUV irradiation at 172 nm. *Langmuir* **2009**, *25* (12), 7129−7134.
(15) Graubner, V.-M.; Jordan, R.; Nuyken, O.; Schnyder, B.; Lippert, T.; Kötz, R.; Wokaun, A. Photochemical Modification of Cross-linked Poly(dimethylsiloxane) by Irradiation at 172 nm. *Macromolecules* **2004**, *37* (16), 5936−5943.
(16) Israëli, Y.; Cavezzan, J.; Lacoste, J. Photo-oxidation of polydimethylsiloxane oils: II—Effect of vinyl groups. *Polym. Degrad. Stab.* **1992**, *37* (3), 201−208.
(17) Dever, J. A.; Banks, B. A.; Yan, L. Effects of Vacuum Ultraviolet Radiation on DC93−500 Silicone. *J. Spacecr. Rockets* **2006**, *43*, 386−392.
(18) Graubner, V.-M.; Jordan, R.; Nuyken, O.; Kötz, R.; Lippert, T.; Schnyder, B.; Wokaun, A. Wettability and surface composition of poly (dimethylsiloxane) irradiated at 172 nm. *Polym. Mater. Sci. Eng.* **2003**, *88*, 488−489.
(19) Ichikawa, S. J. Photooxidation of plasma polymerized polydimethylsiloxane film by vacuum ultraviolet light irradiation in dilute oxygen. *J. Appl. Phys.* **2006**, *100* (3), No. 033510.
(20) Ye, H.; Gu, Y.; Gracias, D. H. Kinetics of ultraviolet and plasma surface modification of poly (dimethylsiloxane) probed by sum frequency vibrational spectroscopy. *Langmuir* **2006**, *22* (4), 1863−1868.
(21) Kogelschatz, U. Dielectric-barrier discharges: their history, discharge physics, and industrial applications. *Plasma Chem. Plasma Process.* **2003**, *23*, 1−46.
(22) Schalk, S.; Adam, V.; Arnold, E.; Brieden, K.; Voronov, A.; Witzke, H.-D. UV-Lamps for Disinfection and Advanced Oxidation - Lamp Types, Technologies and Applications. *IUVA News* **2005**, *8* (1), 32−37.
(23) Joubert, O.; Hollinger, G.; Fiori, C.; Devine, R. A. B.; Paniez, P.; Pantel, R. Ultraviolet induced transformation of polysiloxane films. *J. Appl. Phys.* **1991**, *69*, 6647−6651.
(24) Keller-Rudek, H.; Moortgat, G. K.; Sander, R.; Sörensen, R. The MPI-Mainz UV/VIS Spectral Atlas of Gaseous Molecules of Atmospheric Interest. *Earth Syst. Sci. Data* **2013**, *5*, 365−373.
(25) Lu, H. C.; Chen, H. K.; Chen, H. F.; Cheng, B. M.; Ogilvie, J. F. Absorption cross section of molecular oxygen in the transition E $^3\Sigma_u^-$ v = 0 − $X^3\Sigma_g^-$ v = 0 at 38 K. *Astron. Astrophys.* **2010**, *520*, A19.
(26) Yoshino, K.; Esmond, J. R.; Cheung, A.S.-C; Freeman, D. E.; Parkinson, W. H. High resolution absorption cross sections in the transmission window region of the Schumann-Runge bands and Herzberg continuum of O_2. *Planet. Space Sci.* **1992**, *40* (2−3), 185−192.
(27) Thong-On, B.; Rutnakornpituk, B.; Wichai, U.; Rutnakornpituk, M. Magnetite nanoparticle coated with amphiphilic bilayer surfactant of polysiloxane and poly(poly(ethylene glycol) methacrylate). *J. Nanopart. Res.* **2012**, *14*, 1−12.
(28) Davis, K. M.; Tomozawa, M. Water diffusion into silica glass: Structural changes in silica glass and their effect on water solubility and diffusivity. *Non Crystal Solids* **1995**, *185* (3), 203−220.
(29) Morimoto, Y.; Nozawa, S.; Hosono, H. Effect of Xe_2* light (7.2 eV) on the infrared and vacuum ultraviolet absorption properties of hydroxyl groups in silica glass. *Phys. Rev. B* **1999**, *59*, 4066−4073.
(30) Tsao, M.-W.; Pfeifer, K.-H.; Rabolt, J. F.; Castner, D. G.; Häussling, L.; Ringsdorf, H. Formation and Characterization of Self-Assembled Films of Thiol-Derivatized Poly(Dimethylsiloxane) on Gold. *Macromolecules* **1997**, *30* (19), 5913−5919.

(31) Weldon, M. K.; Marsico, V. E.; Chabal, Y. J.; Hamann, D. R.; Christman, S. B.; Chaban, E. E. Infrared spectroscopy as a probe of fundamental processes in microelectronics: silicon wafer cleaning and bonding Surf. *Sci.* **1996**, *368*, 163−178.
(32) Smith, A. L. Infrared spectra-structure correlations for organosilicon compounds. *Spectrochim. Acta* **1960**, *16*, 87−105.
(33) Bellamy, L. J. *The Infra-red Spectra of Complex Molecules*. Springer Science & Business Media, (2013) ISBN 978−94−011−6019−3 DOI .
(34) Cefalas, A. C.; Sarantopoulou, E.; Gogolides, E.; Argitis, P. Absorbance and outgasing of photoresist polymeric materials for UV lithography below 193 nm including 157 nm lithography. *Microelectron. Eng.* **2000**, *53* (1−4), 123−126.
(35) Hashimoto, Y.; Matsuzawa, S.; Yamamoto, T. Subsurface investigation of the surface modification of polydimethylsiloxane by 172-nm vacuum ultraviolet irradiation using ToF-SIMS and VUV spectrometry. *Surf. Interface Anal.* **2018**, *50* (7), 752−756.
(36) Wu, M. H.; Paul, K. E.; Whitesides, G. M. Patterning Flood Illumination with Microlens Arrays. *Appl. Opt.* **2002**, *41* (13), 2575−2585.
(37) Graubner, V. M.; Nuyken, O.; Lippert, T.; Wokaun, A.; Lazare, S.; Servant, L. Local chemical transformations in poly-(dimethylsiloxane) by irradiation with 248 and 266 nm. *Appl. Surf. Sci.* **2006**, *252* (13), 4781−4785.
(38) Schneider, F.; Draheim, J.; Kamberger, R.; Wallrabe, U. Process and material properties of polydimethylsiloxane (PDMS) for Optical MEMS. *Sens. Actuators A Phys.* **2009**, *151* (2), 95−99.
(39) Fainman, Y.; Lee, L.; Psaltis, D.; Yang, C. *Optofluidics: Fundamentals, Devices, and Applications* 1st ed.; McGraw-Hill Inc.: New York, 2009.
(40) Victoria, M.; Askins, S.; Antón, I.; Sala, G.; Duggan, G. Temperature effects on two-stage optics made of silicone. *AIP Conf. Proc.* **2014**, *1616* (1), 92−96.
(41) Schröer, M.; Scheer, H. C. Insights from evaluation of surface cracks in surface-hardened polydimethylsiloxane by means of video analysis. *J. Vac. Sci. Technol. B* **2021**, *39* (1), No. 013001.
(42) Yamamoto, T. Study on 172-nm vacuum ultraviolet light surface modifications of polydimethylsiloxane for micro/nanofluidic applications. *Surf. Interface Anal.* **2011**, *43* (9), 1271−1276.

https://doi.org/10.1021/acsomega.4c04823
ACS Omega 2024, 9, 45000−45010